

The ISMIP-HOM benchmark experiments performed using the finite-element code Elmer

(1) LGGE CNRS UJF-Grenoble I, France

O. Gagliardini⁽¹⁾ (gagliar@lgge.obs.ujf-grenoble.fr) and T. Zwinger⁽²⁾

(2) CSC-Scientific Computing Ltd., Finland

Introduction

Within the **Ice Sheet Model Intercomparison Project (ISMIP)** the inter-comparison of higher-order models (ISMIP-HOM, coordinated by Frank Pattyn [1]) is addressed to tests that demand a, compared to the shallow ice approximation (SIA), enhanced numerical approach. The FE open source code Elmer [2] solves the complete Stokes equation and hence is well suited for all experiments defined within ISMIP-HOM. Most interesting findings on the results are discussed below.

Governing Equations and Boundary Conditions

continuity: $\nabla \cdot \mathbf{u} = \text{tr} \mathbf{D} = 0$

momentum: $\rho \frac{d\mathbf{u}}{dt} = 2\eta \nabla \cdot \mathbf{D} - \nabla p + \rho \mathbf{g}$,

free surface: $\frac{\partial z_s}{\partial t} + \mathbf{u}_\perp \cdot \nabla_\perp z_s = u_z + a \quad \forall z = z_s(x, y, t)$

slip condition

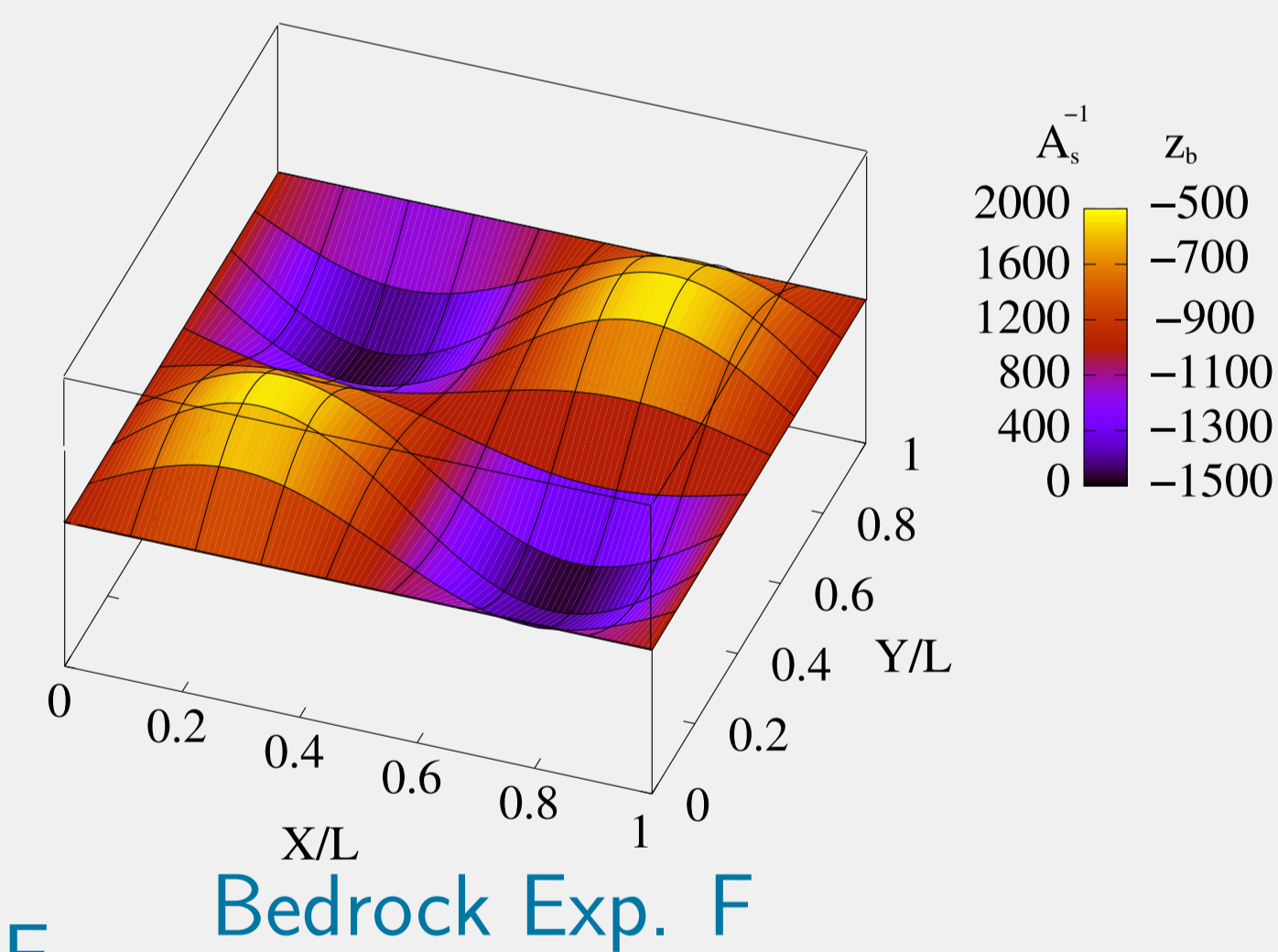
at bedrock: $\mathbf{t}_{x/y} \cdot \mathbf{u}|_b = A_s \tau_{b,x/y}$

Geometry and Boundary Conditions

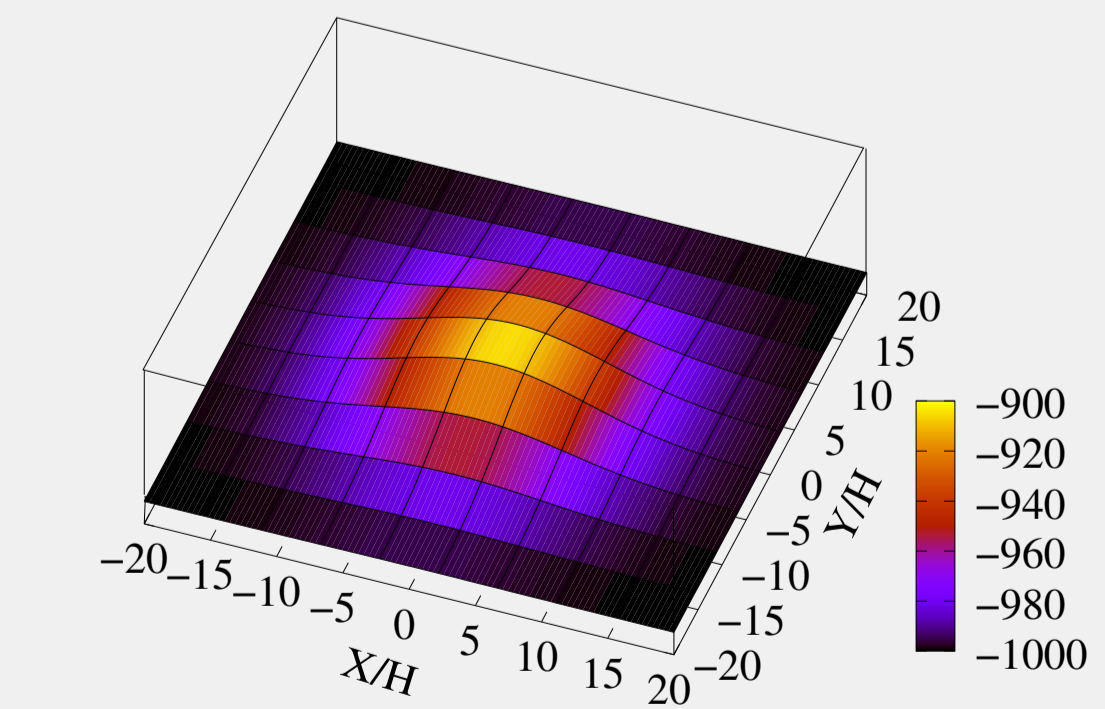
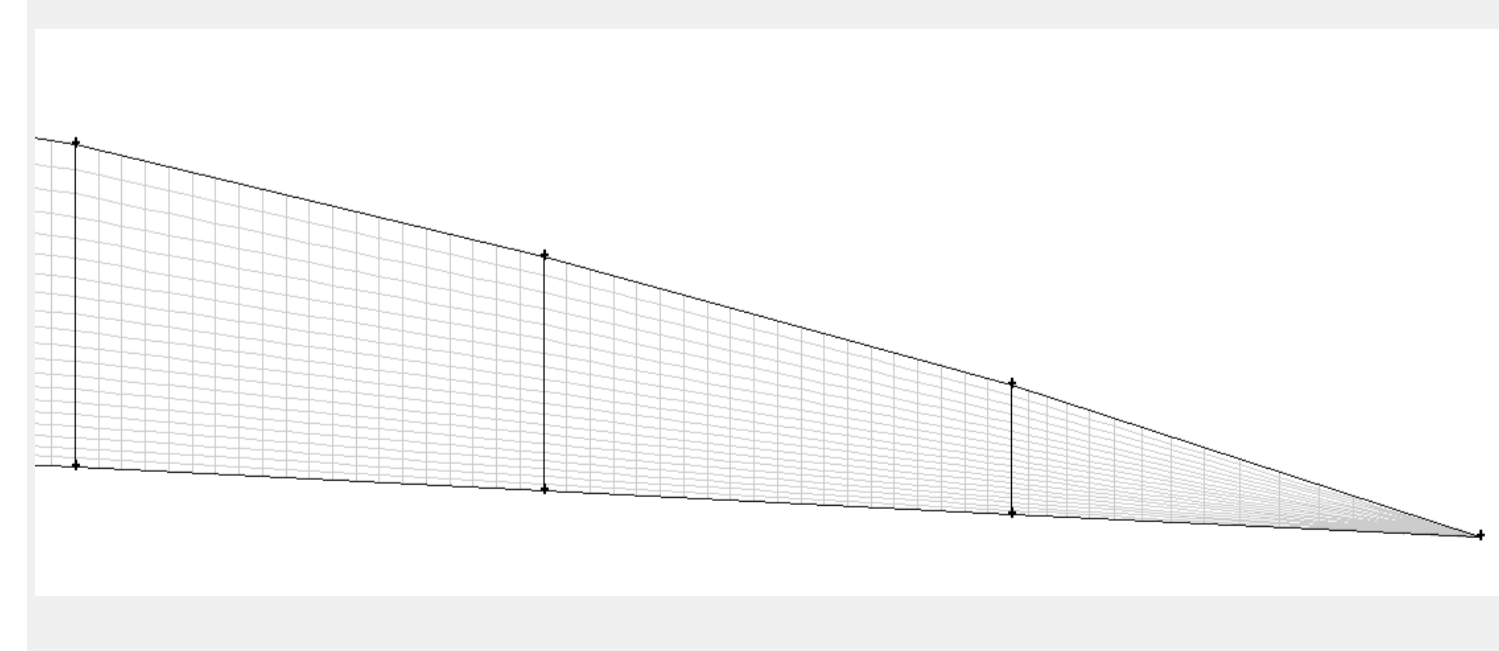
Sinusoidal distribution of the bedrock elevation z_b (Exp. A) and the inverse of the slip coefficient A_s^{-1} (Exp. C)

The corresponding 2d experiments (B and D) evaluate the values at $y/L = 1/4$.

Mesh: layered mesh $60 \times 60 \times 30$, hexahedral elements (Exp. A,C), 240×120 , quadri-lateral elements (Exp. B,D)



Last 3 sections of geometry for Exp. E



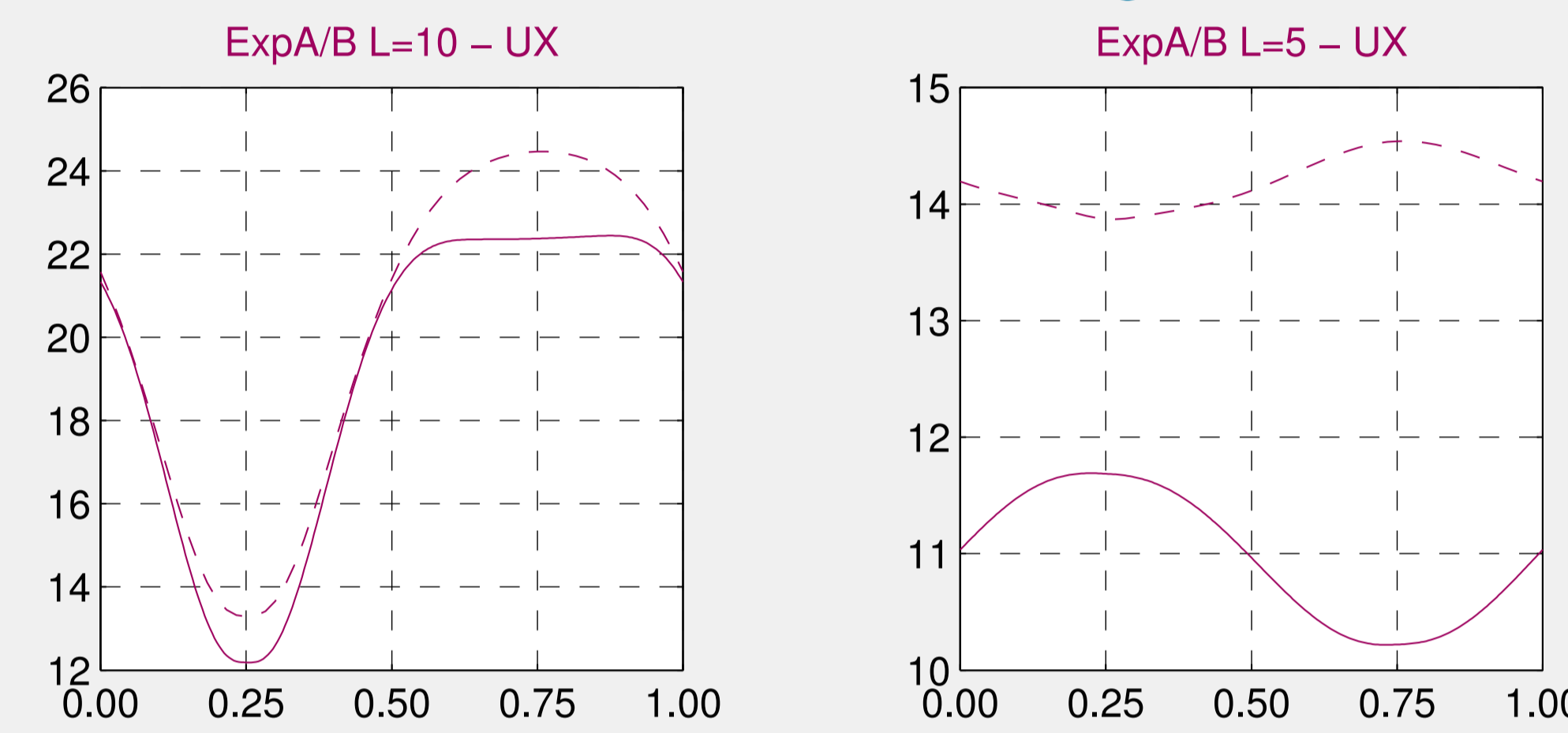
Numerical settings

Stabilization either by Stabilized Finite Elements [3] or Residual Free Bubbles [4].

Linear system solution either iterative using Bi-conjugate Gradient Method [5] or direct by UMFPACK [6]

Experiments A/B (bumpy bedrock)

Comparison between 3d (solid line, Exp. A) and 2d (dashed line, Exp. B) run on sinusoidal bedrock with different wavelengths

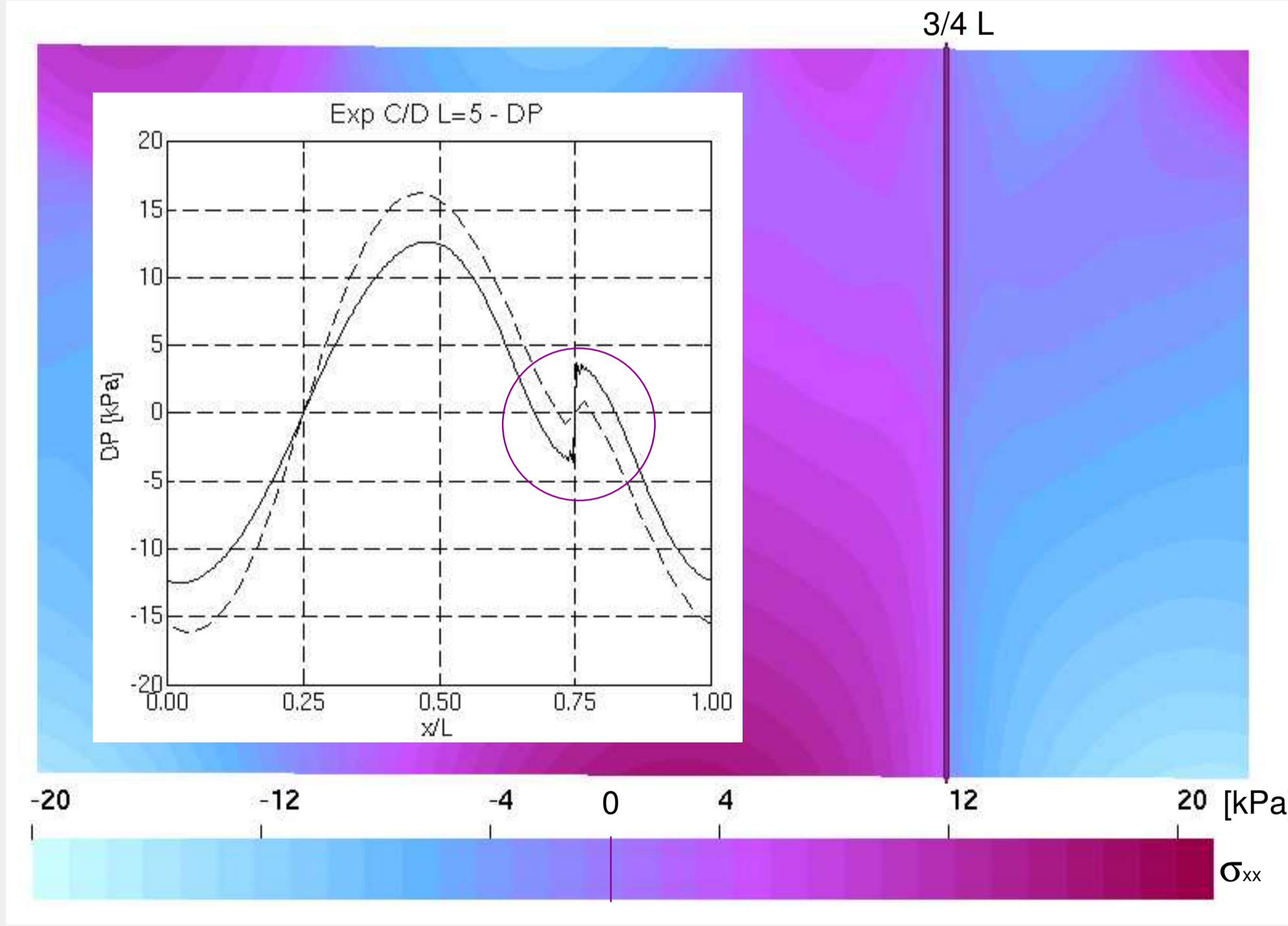


For $L = 5$ km Exp. B shows an increased and to the bedrock elevation anti-correlated downhill velocity (UX). This might be explained that in Exp. B, the displacement at the short wavelength gets too large to be compensated by the vertical flow, thus resulting in higher velocities (mass conservation). This shift in behavior does not occur in Exp. A.

Experiments C/D (ice stream)

Discontinuity of $\Delta p(z_b) = p(z_b) - \rho g H$ (DP) at $x = 3L/4$ (little b/w figure) observed for Exp. C (dashed line) and Exp. D (solid line)

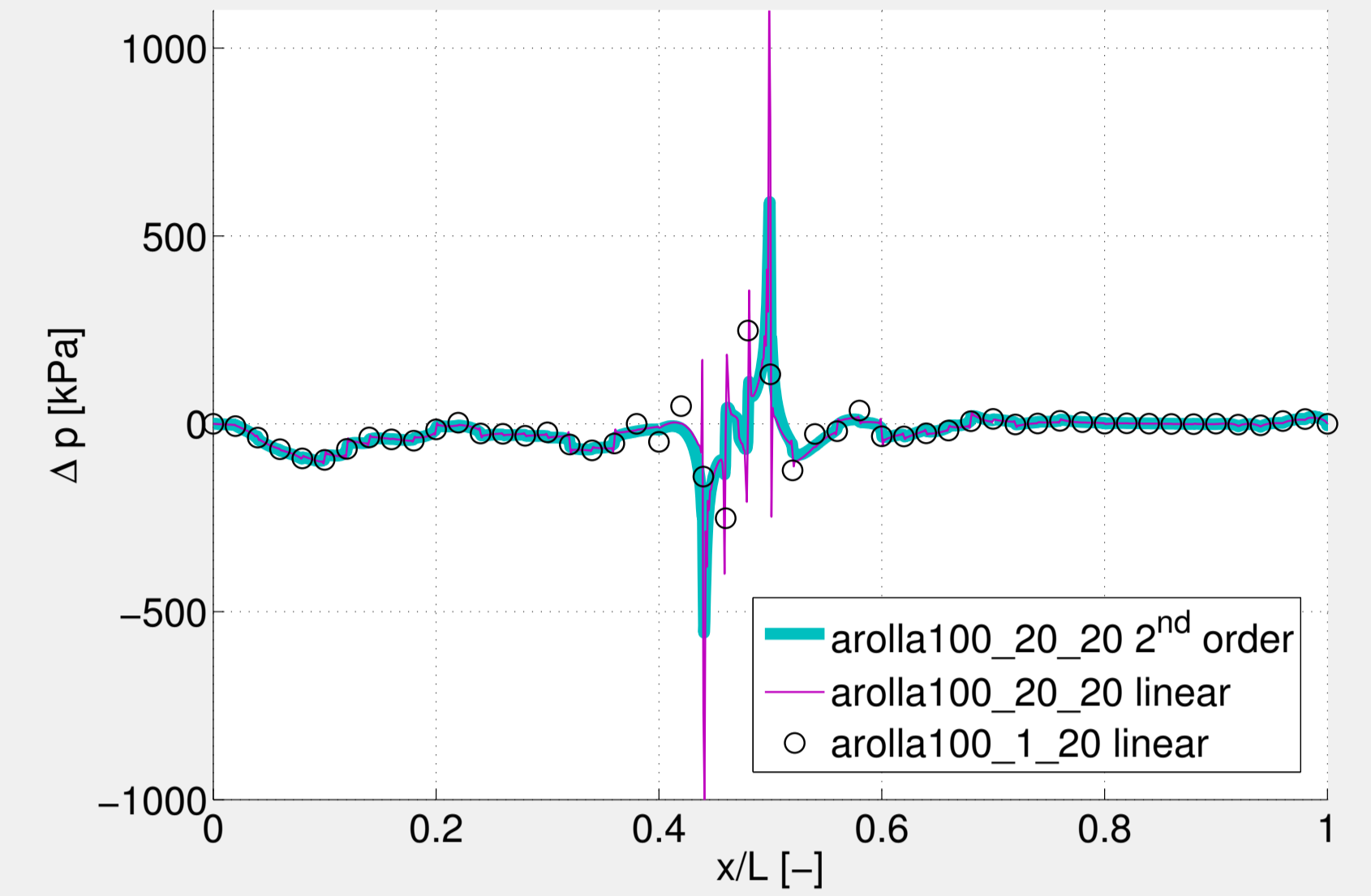
The discontinuity was found for 2d and 3d case and whatever the mesh discretization was. The larger color picture of the deviatoric stress indicates that σ_{xx} changes sign at $x = L/4$ and $x = 3L/4$ from bed to surface, and that its horizontal gradient is very high.



Experiment E (Arolla glacier flowline)

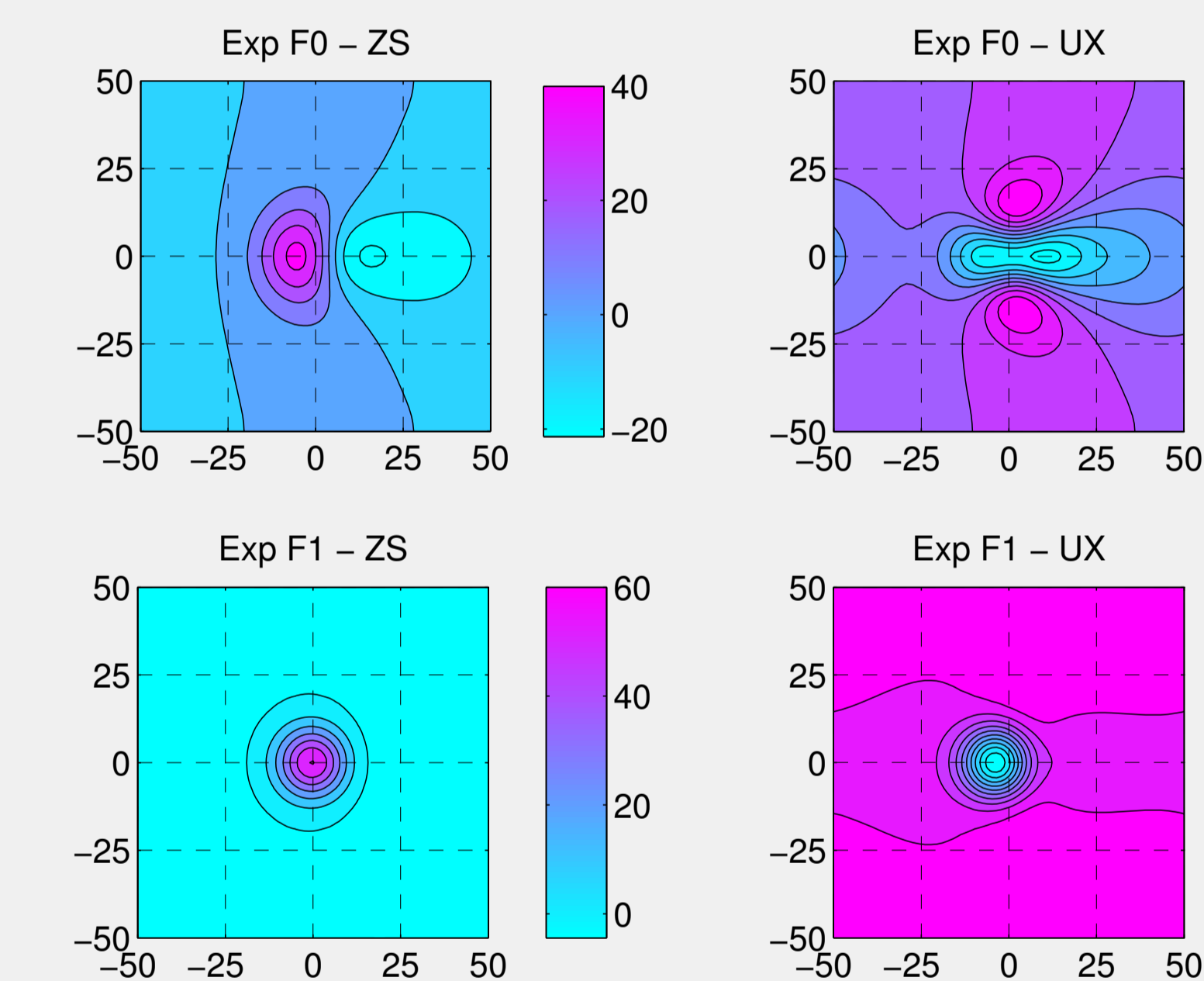
Different oscillatory behavior of the pressure depending on element order

Oscillations in $\Delta p(z_b)$ at the section boundaries (indicated by the circles obtained from a solution on a very coarse grid) occur for runs of Exp. E1 using linear elements (magenta line). The 2nd-order solution, which smears out the discontinuities of the surface normal at the section boundaries, is smooth (cyan line).



Experiment F (free surface flow over bump)

Surface elevation z_s [m] (ZS) and downhill velocity u_x [m a^{-1}] (UX) of the two experiments F0 (upper row) and F1 (lower row)

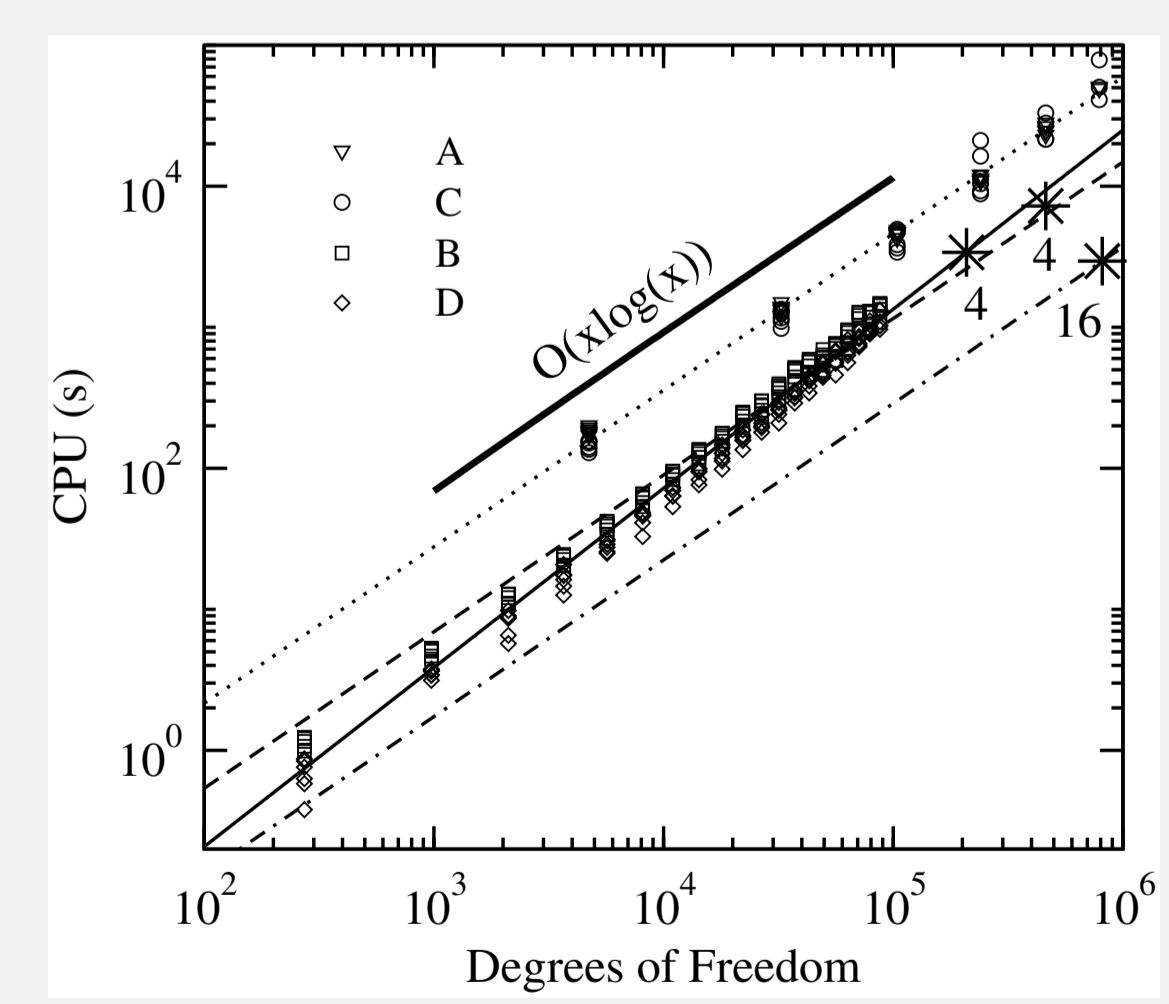


Steady state solution is reached by transient run with steady boundary conditions until change of surface z_s falls below a given numerical threshold. Relative mass-loss in both experiments is within the numerical accuracy and occurs mainly within the first time steps, when temporal gradient dz_s/dt is largest.

Numerical Performance

CPU time consumption vs. degrees of freedom, for experiments A, B, C and D

Power regressions $y = 0.0006x^{1.27}$ (solid) and $y = 0.013x^{1.11}$ (dotted) are inserted (dashed and dash-dot lines parallel to the 3D regression line with exponent divided by 4 and 16). Stars indicate results for parallel runs for experiment A with $L = 5$ km with the annotated number of processors.



Nomenclature: $\mathbf{u} = (u_x, u_y, u_z)^T$...velocity vector, ρ ...mass density of ice, p ...dynamic pressure, \mathbf{D} ...strain-rate, η ...viscosity, t ...time, \mathbf{g} ...acceleration due to gravity, $z_{s/b} = f(x, y)$... z -coordinate of free surface/bedrock, a ...accumulation/ablation, $\mathbf{t}_{x/y}$...tangential vector aligned with x/y -direction at bedrock, A_s ...slip coefficient, $(\bullet)_\perp$...quantity evaluated in $x - y$ plane only, $(\bullet)_{s/b}$...evaluated at free surface/bedrock

download: http://staff.csc.fi/zwinger/data/egu2007_poster.pdf

References:

- [1] <http://homepages.ulb.ac.be/~fpattyn/ismip>
- [2] <http://www.csc.fi/elmer>
- [3] Franca, L. P., Frey, S. L., and Hughes, T. J. R. (1992). Stabilized finite element methods [...]. *Comput. Methods Appl. Mech. Eng.*, 95:253–276.
- [4] Baiocchi, C., Brezzi, F., and Franca, L. P. (1993). Virtual bubbles and the Galerkin least squares method. *Comp. Meths. Appl. Mech. Engrg.*, 105:125–141.
- [5] Kelley, C. (1995). *Iterative methods for linear and nonlinear equations*. Frontiers in Applied Mathematics, 16, SIAM.
- [6] Davis, T. A. (2004). A column pre-ordering strategy for the unsymmetric-pattern multifrontal method. *ACM Trans. Math. Software*, 30(2):165–195.